

1 **Optimization of a hydrometric network extension using specific flow, kriging and**
2 **simulated annealing**

3 **Afef Chebbi^{1,2} , Zoubeida Kebaili Bargaoui¹ , Nesrine Abid¹ and Maria da Conceição**
4 **Cunha³**

5 ¹ Université de Tunis El Manar, Ecole Nationale d’Ingénieurs de Tunis, BP 37 1002 Tunis, Tunisia

6 ² Université de Sousse, Institut Supérieur des Sciences Appliquées et Technologie de Sousse, Cité Taffala (Ibn Khaldoun), 4003 Sousse,
7 Tunisia

8 ³ Civil Engineering Department, University of Coimbra Polo II da Universidade-Pinhal de Marrocos, 3030-290 Coimbra, Portugal

9

10 **Abstract**

11 In hydrometric stations, water levels are continuously observed and discharge rating curves
12 are constantly updated to achieve accurate river levels and discharge observations. An
13 adequate spatial distribution of hydrological gauging stations presents a lot of interest in
14 linkage with the river regime characterization, water infrastructures design, water resources
15 management and ecological survey. Due to the increase of riverside population and the
16 associated flood risk, hydrological networks constantly need to be developed. This paper
17 suggests taking advantage of kriging approaches to improve the design of a hydrometric
18 network. The context deals with the application of an optimization approach using ordinary
19 kriging and simulated annealing (SA) in order to identify the best locations to install new
20 hydrometric gauges. The task at hand is to extend an existing hydrometric network in order to
21 estimate, at ungauged sites, the average specific annual discharge which is a key basin
22 descriptor. This methodology is developed for the hydrometric network of the transboundary
23 Medjerda River in the North of Tunisia. A Geographic Information System (GIS) is adopted
24 to delineate basin limits and centroids. The latter are adopted to assign the location of basins
25 in kriging development. Scenarios where the size of an existing 12 stations network is
26 alternatively increased by 1, 2, 3, 4 and 5 new station(s) are investigated using geo-regression
27 and minimization of the variance of kriging errors. The analysis of the optimized locations

28 from a scenario to another shows a perfect conformity with respect to the location of the new
29 sites. The new locations insure a better spatial coverage of the study area as seen with the
30 increase of both the average and the maximum of inter-station distances after optimization.
31 The optimization procedure selects the basins that insure the shifting of the mean drainage
32 area towards higher specific discharges.

33 **Keywords** hydrological gauging stations; network optimization; geo-regression; ordinary
34 kriging; simulated annealing

35 **1. Introduction**

36 A hydrometric network is aimed at giving the hydrological information to be used for
37 ecological survey, hydrological survey, hydrological regionalization as well as infrastructures
38 design. Flood estimates are of major importance since they are needed for designing civil
39 engineering works, inundation risk zoning and an estimation of ecological flows. Both water
40 source infrastructure design and management (reservoirs, water distribution systems,
41 irrigation networks, etc.) are based on flood estimation. Due to the increase of riverside
42 population and the associated flood risk issues, the hydrological networks need to be
43 developed.

44 According to Mishra and Coulibaly (2009), a hydrometric network should be optimized to
45 collect most hydrological information and in the most precise way. More generally, the
46 commonly used processes for network optimization include statistical approaches, a user
47 survey procedure, a hybrid approach, and sampling plans (Vivekanandan, 2012). *Statistical*
48 *approaches* for hydrometric network optimization range from clustering methods (Bum and
49 Goulter, 1991) and spatial regression (Tasker and Stedinger, 1989) to entropy-based
50 techniques (Caselton and Husain, 1980). *Clustering methods* are usually used to identify
51 groups of hydrometric gauging stations with similar flow characteristics on the basis of a
52 similarity matrix defining the similarity of each station to every other station. This constitutes

53 an important step in the network design procedure. The annual average runoff is a main flow
54 characteristic and spatial regression is often used to predict it at ungauged locations (Daigle et
55 al., 2011). *Entropy methods* may also assist network design by quantifying the relative
56 information content and by estimating uncertainty (Vivekanandan, 2014). Moreover, the *User*
57 *survey procedure* is based on the users' needs to continue or discontinue stations depending
58 upon the type of data needed in the basin. This investigation by its nature relies on a certain
59 amount of personal decisions (Davar and Brimley, 1990).

60 *The hybrid method* combines models by adopting the output from one method as an input into
61 another model for network optimization. For example an algorithm of numerical optimization
62 permits to improve the optimal network design by variance reduction and allows the insertion
63 of other criteria in the objective function such as the economic cost of the data collection
64 (Mishra and Coulibaly, 2009). *Hydrologic sampling* plans are based on the influence of
65 rainfall on stream flow processes. The effectiveness of sampling plans is evaluated by the
66 variance of error in the estimate stream flow (Tarboton et al., 1987).

67 On the other hand, the rainfall network design is often achieved by using the kriging
68 interpolation method combined with optimization algorithms such as simulated annealing (see
69 for example Barca et al., 2008; Chebbi et al., 2013). Kriging has also been used for
70 piezometric networks optimization. For instance, Rouhani (1985) used two criteria for
71 piezometric network optimization: the first concerns the reduction of the kriging variance
72 while the second is related to the expected economic gain, measured by loss reduction. One
73 fundamental upshot of kriging is that it results in the estimation of the variance of
74 interpolation errors, making it possible to evaluate network performance. Whereas entropy
75 method is worth for existing networks, the kriging interpolation method may be extended for
76 planned networks. Kriging often employs a semivariogram function representing the structure
77 of the spatial variability of the data. The semivariogram effectively gives the same

78 information as an auto-correlation function. However, it has a big advantage of being an
79 unbiased estimator as it does not depend on the mean of the data set. So, it is proposed here to
80 get profit of the kriging approaches in order to improve the design of a given hydrometric
81 network. The main difficulty here resides in defining a suitable hydrometric study variable
82 and a suitable objective function, as well in addition to a suitable kriging method.

83 In this study, we have adopted a specific discharge as a prime study variable representing the
84 ratio of the river discharge to the drainage area and which is also called average specific
85 annual module. For a long time in flood studies, the record specific discharges are adopted as
86 a key variable to obtain regionally-developed curves (Castellarin, 2007). So, a specific
87 discharge is considered here as a key watershed descriptor.

88 There are many other ways to handle the issue of hydrometric network optimization since the
89 hydrologic response is multidimensional. Therefore, instantaneous hydrograph responses to
90 rainfall events are described by at least three variables: flood duration, flood peak and flood
91 volume. An objective function including these variables may be achieved but we cannot rely
92 on this approach because of data limitations. We have no information about the flood series
93 (except at daily resolutions). Basins have signatures which can be described by using some
94 statistics of the basis of the flow-duration curve (Sadegh et al., 2016) obtained by analyzing
95 daily discharges. These above-mentioned statistics may be used to optimize the hydrometric
96 network. The only statistics adopted here is the sample mean of annual discharges. We did not
97 apply other statistics even though they would be a possible extension of the current work. The
98 Runoff coefficient is another basin signature which can be adopted to solve the optimization
99 of hydrological networks. The difficulty with basin runoff coefficient is that it involves the
100 estimation of the basin average rainfall, which in turn is a “rainfall product” that needs
101 interpolation tools in order to be evaluated. Another alternative is the use of digital models
102 (based on a Geographic Information System) associated to soil, land use information and

103 classification methods to find the most representative basins. The advantage of not adopting
104 such an alternative is to limit the need of implementing digital models which themselves are
105 to be verified using in situ data.

106 Thus, this work intends to extend the use of a specific river discharge, as a study variable to
107 the hydrometric network optimization. One implicit assumption is that the geographic regions
108 in the study are hydrologically homogeneous.

109 Many basin attributes may be included as a proxy for flood (and the specific discharge)
110 estimation. They are often adopted in geo-regression approaches. The drainage area, the basin
111 geology together with land use descriptors, soil characteristics, elevation data, and climate
112 variables such as mean annual precipitation are often proposed as flood proxy or surrogates
113 (Acreman and Sinclair, 1986). Wilson and Gallant (2000) noticed that steepness can be
114 considered as a surrogate for overland and subsurface flow velocity and the runoff rate.
115 Hundedcha and Bardossy (2004) adopted basin size, slope and shape as characteristics for
116 regionalizing Hydrologiska Byrans Vattenbalansavdelning (HBV) rainfall runoff model
117 parameters. Kjeldsen and Jones (2007) adopted both the drainage area and the average annual
118 rainfall together with an index of flood reduction attributable to reservoirs and lakes and a
119 derived base flow index using the Hydrology of Soil Type classification.

120 Here, the drainage area, which is the most commonly used variable in the literature, is
121 adopted as a proxy variable for the estimation of the specific module, similarly to Kron and
122 Willems (2002) who consider only the drainage area as proxy for flood discharge for a large-
123 scale flood hazard mapping. However, another alternative linking basin runoff to mean basin
124 precipitation is tested. The ordinary kriging estimation involves the basin centroid inter-
125 distances. Topological kriging (or top-kriging) is recently proposed as an alternative to
126 ordinary kriging. It is based on regularized semivariograms between catchments which are
127 estimated on the basis of point semivariograms and the distances between basin centroids and

128 drainage areas are assumed as a proxy. The main difference is that top-kriging takes into
129 account the nested nature of catchments by considering that the area is shared by two
130 catchments. Yet, top-kriging requires a very large computation time compared to ordinary
131 kriging. Laaha et al. (2014) found that for locations without upstream data points, the
132 performances of the two methods are similar. Their study resulted in coefficients of
133 determination in cross-validation that are 0.75 for the top-kriging and 0.68 for regional
134 regression methods, including nested basins. A major interest of the top-kriging method is its
135 ability to estimate (and allow to visualize) continuously the spatial variability of the specific
136 flow over the whole hydrographic network. Nevertheless, in this study, we do not need to
137 continuously estimate the specific flow rate. Therefore, in our opinion, the small gain in terms
138 of explanatory power does not justify such an investment in computation time, especially that
139 the kriging procedure is repeated as many times as it is necessary to optimize the objective
140 function.

141 Thus, the approach using ordinary kriging is selected as an alternative. It is also achieved in
142 order to take advantage of the numerical tools developed so far by the authors in previous
143 studies (Chebbi et al., 2011).

144 To assign a geographical distance between basins (in semivariogram analysis and kriging
145 estimation), the Euclidian distance between the basin's centroids is often adopted (see for
146 example Daviau et al., 2000; Adamowski and Bocci, 2001; Eaton et al., 2002; Skøien et al.,
147 2003). In fact, it is not possible to consider the basin outlets for distance estimation because
148 the runoff is a response of the basin as a whole. Some variables other than the geographic
149 location by such as a basin mean altitude, basin slope, and basin mean annual precipitation
150 can be adopted to build the distances between basins but for the reasons advocated above
151 (lack of data availability), this is out of the scope of this study.

152 The main purpose of this study is to identify an optimal set of new locations to upgrade the
153 size of an initial hydrometric network. The objective addressed in stating the optimization
154 problem is to make a more accurate evaluation of the average specific annual module.

155 The new contribution of this study is really to find a substitution variable for the runoff which
156 is not suitable for the use of kriging because it is not an additive variable. The problem is
157 solved by using the transformation of the runoff into an effective rainfall (by using the ratio of
158 runoff and the drainage area which corresponds to the specific discharge) and also by using a
159 scaling formula (geo-regression) allowing a basin runoff inter-comparison.

160 The case study concerns the hydrometric network of the transboundary Medjerda River, in
161 Northern Tunisia. This study area is selected because the Medjerda represents the main river
162 in Tunisia with a 350 km length. The drainage area of the basin at the Mediterranean outlet in
163 Kallat Landlous is about 23 500 km². Another reason for which this study area is chosen
164 relies in taking advantage of the long series of runoff observations available in this basin for a
165 long time (Rodier et al., 1981). This insures a good accuracy in the estimation of the mean
166 annual runoff.

167 Section 2 presents the methods used in this paper. Section 3 presents the study area and data
168 while Section 4 sets out the obtained results. The concluding remarks are presented in Section
169 5.

170 **2. Methods**

171 The methods adopted in the current work are divided into three main topics: data mining,
172 ordinary kriging and statement of the optimization problem.

173 **2.1 Data mining using geo-regression**

174 The analysis adopts (a) the average specific annual module as a primary study variable; (b)
175 the coordinates of basin centroids as a basis to estimate the spatial variability structure,
176 similarly to Merz and Blöschl (2005) (c) the drainage area as the proxy of a specific runoff.

177 The method requires defining a number M of evaluation basins and a number C of candidate
 178 basins as well a set of initial guesses. Because the M evaluation basins, the C candidate basins
 179 and the initial controlled basins are of various sizes, it is necessary to reduce the scale effect
 180 of drainage area. Assuming that the average specific annual module for a basin of size A_N is
 181 Q_N and assuming the scaling relationship $Q_N/Q=(A_N/A)^\beta$, the average specific annual module
 182 Q is replaced by the standardized specific module Q_N following Merz and Blöschl (2005) who
 183 adopted $A_N= 100$ km². It comes:

$$184 \quad Q_N = \left(A A_N^{-1} \right)^\beta Q \quad (1a)$$

185 where Q_N is the average specific annual module for a hypothetical 100 square km basin, A
 186 (km²) the gauged drainage area and Q is the observed average specific annual module. The
 187 scaling exponent β is found by a regression analysis between $\log(Q_N)$ and $\log(A)$. In Skøien et
 188 al. (2006), fitting resulted in $\beta=-0.33$ for mean annual discharge for Austria. To estimate β ,
 189 several values are tested. Logarithmically transformed specific discharges are plotted as a
 190 function of the logarithm of drainage area for each tested β value to help verifying the model
 191 adequacy visually. Besides, the regression coefficient of determination R^2 is assumed as a
 192 quality criterion. Other criteria such as Root Mean Square Errors (RMSE) (Fair, 1986) or
 193 Akaike Information Criteria (AIC) (Bozdogan, 2000) can be assumed for model evaluation.
 194 However, R^2 is selected as an alternative to RMSE for it is dimensionless. The use of AIC is
 195 not needed because the number of parameters to be estimated is fixed regardless of the model
 196 (It is β which is to be estimated).

197 Moreover, the alternative of linking mean basin runoff to mean basin rainfall instead to
 198 drainage area is tested. A model similar to Eq. (1a) is proposed.

$$199 \quad Q_N = \left(P P_{ref}^{-1} \right)^\beta Q \quad (1b)$$

200 where Q_N is the average specific annual module for a hypothetical reference rainfall of 100
201 mm, P (mm) the mean annual basin rainfall, P_{ref} (mm) is a reference rainfall and Q is the
202 observed average specific annual module.

203 The best model (Eq. (1a) or Eq. (1b)) is finally selected on the basis of the performance
204 measure R^2 .

205 **2.2 Interpolation using ordinary kriging**

206 Kriging is a spatial interpolation method which takes into account the spatial variability of the
207 data. This interpolation method is an unbiased estimator where the kriging (interpolation)
208 error variance is minimized (Matheron, 1970). The basic idea of Euclidian kriging methods
209 (such as ordinary kriging) is to estimate the value of a regionalized variable Z by a linear
210 combination of the neighboring observations. Here, the neighboring observations are the
211 basins which are “close” with respect to their centroid location when considering the
212 prediction error Z of the fitted regression as a kriging variable.

213 The semivariogram is the structure function used here to model variability associated with the
214 regionalized variable, Z . It measures the spatial variability of squared differences between
215 pairs of variables, which allows building the experimental semivariogram, $\gamma(h)$, given by:

$$216 \quad \gamma(h) = \frac{1}{2N(h)} \sum_{i=1}^{N(h)} [Z(x_i + h) - Z(x_i)]^2 \quad (2)$$

217 where x_i and x_i+h are two sampling locations separated by a distance h , $N(h)$ represents the
218 number of sample points using h , $Z(x_i)$ and $Z(x_i+h)$ represent values of the variable Z
219 measured at both locations. In this study, the basin centroids are adopted to locate basin
220 sampling locations and determine the lags h as reported in Merz and Blöschl (2005). They are
221 estimated by using GIS as reported in the Data section. The variable Z is related to the
222 average specific annual discharge.

223 A semivariogram model is fitted to the experimental semivariogram. The fitted
 224 semivariogram is characterized by three main parameters: range, sill, and nugget. ‘Range’
 225 represents the distance limit beyond which the data are no longer correlated. ‘Sill’ represents
 226 the variable variance. The ‘Nugget’ effect is a random component of the field Z and it
 227 represents either measurement errors or the variation of the studied variable at a small scale
 228 (Cressie, 1993).

229 Two semivariogram models are used here as alternatives: exponential and spherical. The
 230 exponential model for the semivariogram is given by Eq. (3):

$$231 \quad \gamma(h) = \omega * [1 - \exp(-h/a)] + \omega_0 \quad (3)$$

232 where ω is the structural variance, ω_0 is the nugget variance and a is the range parameter. In
 233 the case of the exponential model, the range is defined as the distance at which the
 234 semivariogram is of 95% of the sill. So, it is equal to $3a$ according to Eq. (3). The sill is equal
 235 to $(\omega + \omega_0)$ (Bardossy, 1997).

236 The spherical model for the semivariogram is given by Eq. (4):

$$237 \quad \gamma(h) = \omega * [1.5 * (h/a) - 0.5 * (h/a)^3] + \omega_0 \quad (4)$$

238 Ordinary kriging is furthermore adopted. Thus, the estimated value $Z^*(x_0)$ at a location x_0 is a
 239 weighted linear combination of observations x_i at neighboring gauged basins $i=1, N_{nb}$ where
 240 N_{nb} is the number of observations within the exploring neighbourhood (Matheron, 1970):

$$241 \quad Z^*(x_0) = \sum_{i=1}^{N_{nb}} \lambda_i Z(x_i) \quad (5)$$

242 where $Z^*(x_0)$ is the estimated value of Z at the ungauged location x_0 , λ_i is the weight given to
 243 the observation at the location x_i .

244 The variable Z in Eq. (2) and Eq. (5) is stated as the error (or regression residual) between the
 245 logarithms of the observed Q_N and the logarithms of the estimated Q_N by the regression model
 246 of Eq. (1a) or Eq. (1b).

247 The kriging weights λ_i are estimated as the solution of the ordinary kriging system (Eq. (6)):

$$248 \begin{cases} \sum_{i=1}^{N_{nb}} \lambda_j \gamma(x_j - x_i) + \mu' \\ = \gamma(x_j - x_0) \quad j = 1, \dots, N_{nb} \\ \sum_{i=1}^{N_{nb}} \lambda_i = 1 \end{cases} \quad (6)$$

249 where μ' is a Lagrange parameter accounting for the constraints on the weights (their sum is
 250 equal to unity). The x_j and x_i are the coordinates of the basin centroids, and $\gamma(x_j - x_i)$ is the
 251 estimated semivariogram for the lag between basin centroids x_j and x_i , using the theoretical
 252 semivariogram model. Thus, the weights λ_i and the Lagrange parameter μ depend entirely on
 253 the semivariogram model.

254 The kriging variance σ_0^2 helps to define and quantify the optimization objective function
 255 (Cressie, 1993; Barca et al., 2008). It is expressed for any ungauged location x_0 using the
 256 semivariogram model by:

$$257 \sigma_0^2 = \gamma(0) - \sum_{i=1}^{N_{nb}} \lambda_i \gamma(x_i - x_0) - \mu' \quad (7)$$

258 As stated earlier, the sample semivariogram is fitted to an exponential model and to a
 259 spherical model. The model parameters are evaluated by manual calibration. In fact, the first
 260 guess for each parameter is graphically adjusted. The acceptability of the fitted semivariogram
 261 model is then tested through the leave-one-out cross-validation scheme. This method removes
 262 a single data point, just one at a given time, and it estimates the result at the now missing
 263 location. The quality of the prediction is then evaluated. The parameter values are thus
 264 modified in order to obtain the best cross-validation results. The leave-one-out cross-
 265 validation is considered as one of the most commonly used methods to make an informed
 266 decision as to which model will provide the best predictions (Lin and Chen, 2004).

267 The standardized error and the coefficient of determination are adopted as criteria to evaluate
268 the cross-validation results. The standardized error is equivalent to the value of the residuals
269 between the observed values and the kriged Z^* values, divided by the standard deviation of
270 kriging errors (Glatzer and Muller, 2004). Standardized residuals which are more than 2 and
271 less than -2 are usually considered too large and, consequently, the parameters of the model
272 semivariogram are modified in order to insure an acceptable range for the standardized
273 residuals. The coefficient of determination (R^2) is also used for cross-validation (Laaha et al.,
274 2014).

275 After performing the selection and validation of the fitted semivariogram model, the
276 dependency ratio, which represents the percentage of the nugget effect (ω_0) in relation to the
277 sill ($\omega + \omega_0$), is determined according to Cambardella et al. (1994). This ratio is used to
278 interpret the strength of the dependency reported by the semivariogram structure. The higher
279 the ratio is, the higher is the independency of the field observations. The values of
280 dependency ratio are grouped and interpreted as follows: high dependency (< 25%), moderate
281 dependency (25% - 75%), and low dependency (> 75%).

282 ***2.3 Statement of the optimization problem***

283 *2.3.1 Network design problem: Minimizing the average kriging variance*

284 The problem statement is to extend an existing hydrometric network in order to evaluate the
285 average specific annual module more accurately in the study basin. Thus, the optimization
286 problem consists in minimizing an objective function defined here as the average kriging
287 variance of error over a fixed evaluation grid, composed by $i=1, M$ evaluation basins. This
288 criterion, based on the geostatistical estimation error, is mentioned by Cressie (1993) among
289 the criteria to adopt in network design problems:

$$290 \quad OF = \sum_{i=1}^M \sigma_i^2 / M \quad (8)$$

291 This objective function depends entirely on the semivariogram model and on the M selected
292 grid points. The collection of the M centroids constitutes what is called the “grid nodes”. For
293 kriging implementation, these evaluation basins are required to be different from the
294 controlled basins.

295 Thus, when a “grid” of M basins is adopted to compute the variance of kriging error and
296 quantify the objective function OF , the minimization problem is solved by using a simulated
297 annealing algorithm (Kirkpatrick et al., 1983). Indeed, the simplicity of the algorithm and the
298 variety of optimization problems to which the algorithm is used are among the main
299 advantages of simulated annealing (Fleischer, 1995). This algorithm is applied in Cunha
300 (1999) for solving aquifers' management problems. It was also applied by Chebbi et al. (2011)
301 in order to optimize the selection of rainfall stations in the issue of increasing the size of an
302 existing rainfall network.

303 ***2.3.2 Definition of candidate solutions and simulation scenarios***

304 The optimal locations are chosen from the C candidate stations which are represented by the
305 centroids of their drainage area. The candidate stations are selected in such a way that they
306 cover the whole study region. Besides, they are selected in such a way that they do include
307 outlets representing upstream basins, and small to moderate size basins. Moss and Tasker
308 (1991) recommended that the number of candidate stations should be at least three times the
309 number of the desired optimal stations. In this work, due to the high cost of the hydrometric
310 equipments and to the financial constraints, we seek to implement only one to five new
311 stations. Thus, the new locations investigated by using the SA optimization scheme for five
312 scenarios respectively involve: (1) a network consisting of 13 hydrometric gauges, (2) a
313 network consisting of 14 hydrometric gauges, (3) a network consisting of 15 hydrometric
314 gauges, (4) a network consisting of 16 hydrometric gauges, and (5) a network consisting of 17
315 hydrometric gauges, including all $N=12$ existing stations. The same 15 candidate locations are

316 investigated for the five scenarios in order to allow for an inter-comparison scenario,
317 whatever the final size of the optimized network.

318 **3. Study area and data**

319 The study area is the North of Tunisia, including the Medjerda basin (BV5), the Northern
320 Coast Basin (BV3) and the Cap Bon – Méliane Basin (BV4). However, the optimization has
321 been performed for the Medjerda Basin (BV5) which covers an area of 21,000 km² in Tunisia.
322 Figure 1 shows the hydrometric network of the study area composed of 19 controlled basins.
323 Their names and drainage areas are reported in Table 1. Twelve out of the 19 controlled
324 basins are located in Medjerda Basin (BV5) and the remaining are in its neighboring basins.
325 Six stations are located in the North Coast Basin (BV3) and one single station is part of the
326 Cap Bon – Méliane Basin (BV4). Neighboring basins belonging to BV3 and BV4 are used
327 both for developing the spatial variability assessment during the sample semivariogram
328 estimation and for kriging in the cross validation step. In addition to the twelve stations
329 studied in Medjerda Basin (BV5), two other stations are located in the Tessa sub basin but are
330 not included in the sample. They are Pont Route Souani on Oued Souani, a tributary of Tessa
331 and Sidi Mediane on Oued Tessa. The reason is that the observed average annual modules of
332 these two stations have singularities. In addition, Oued Souani is already controlled by a dam
333 achieved since 2005. This is why these two stations are not taken into consideration in the
334 initial hydrometric network of Medjerda.

335 In this work, all basin boundaries are derived from a digital elevation model available within a
336 30-meter resolution (ASTER, 2012). Furthermore, the coordinates of the basin centroids are
337 derived from the resulting basin boundaries using ArcGIS. Sizes of the 12 gauged basins of
338 the Medjerda basin range from 60 to 20811 km².

339 A brief description of the Medjerda tributaries is required to understand the motivation that
340 lies behind the selection of the *M* evaluation basins (grid nodes) and the *C* candidate basins.

341 In the right bank of the Medjerda river, (viewed from upstream direction), the main direct
342 tributaries are Oued (river) Mellegue which is partly situated in Algeria, Oued Tessa, Oued
343 Siliana and Oued Lahmar. On the left bank, the main tributaries are Oued Rarai, Oued
344 Bouheurtma, Oued Kasseb, Oued Beja and Oued Zerga. Oued Mkhachbia is a very small
345 basin neighboring Oued Beja. Tributaries of the right bank are much longer and steeper than
346 those of the left bank and they are much subjected to water erosion. On the other hand, some
347 of the right bank tributaries, such as Rmil, a tributary of the Siliana river and Rmel, a tributary
348 of the Mellegue river, are responsible for intense floods (Rodier et al., 1981; Ghorbel, 1997;
349 Zahar et al., 2008). Thus, the selection of M and C basins requires considering the basin
350 location: left bank or right bank.

351 Table 1 displays the observed average annual module which is reported by using the National
352 hydrological service (DGRE) annual reports. Figure 1 and Table 1 show that there is a lack in
353 the observation of upstream sub basins of the Medjerda River. Indeed, historically speaking,
354 this network is aimed to design the existing large dams. Besides, it is intended for flood
355 forecasting purposes. This might explain why small basins are left aside in the current
356 network conception. Thus, network size augmentation may help to correct this kind of bias in
357 the drainage area coverage. So, the selection of M and C basins needs to include basins of
358 small and moderate sizes.

359 Because we deal with one to five new sites, it is assumed that $M=20$ is sufficient to compute
360 the grid average kriging error with confidence. The sampling of evaluation grid basins is
361 conceived in such a way as to cover the study domain (in both left and right banks) and to
362 include small, moderate and large drainage areas. Figure 2 shows the “grid” node locations of
363 the $M=20$ basins selected for the evaluation of the objective function. On the other hand, for
364 the purpose of successively selecting one to five new basins to be controlled, 15 candidate
365 locations are selected (Figure 3). Similarly, candidate stations are chosen on either the right or

366 the left bank. For example, for Tessa basin on the right bank, two candidate sites (C2 and
367 C14), are prospected respectively upstream and downstream of an important river recharge
368 area (Figure 3). For Zerga basin on the left bank, two candidate sites are also proposed (C9
369 and C10) as their tributaries meet at a confluence (Figure 3). Table 2 reports the basin size
370 and the tributary of the 15 candidate stations as well as the description of the reason of their
371 selection. As needed to improve the network cover for small and moderate basins sizes, the
372 candidate drainage areas vary from 107 to 755 km².

373 To adjust the geo-regression parameter β , when using the drainage area as attribute (Eq. (1a)),
374 a network of 39 well-documented gauged basins belonging to the National hydrometric
375 network of Tunisia is considered. Their sizes vary from 3 to 20811 km². Their average annual
376 modules vary between 0.05 and 27.5 m³/s. The plot of the logarithms of the observed average
377 specific annual module versus the logarithms of the drainage area is reported in Figure 4
378 where the 19 basins of Northern Tunisia are made distinguishable from the whole sample of
379 39 basins. For the other alternative of linking mean basin runoff to the mean basin rainfall
380 (Eq. (1b)), only a subgroup of 21 gauged basins, among the existing 39 ones, is used to adjust
381 the geo-regression parameter β . In fact, mean annual rainfall data are available only for these
382 21 stations.

383 **4. Results**

384 **4.1 Scaling and regression results**

385 The scaled specific discharge Q_N sample (Eq. (1a)) is estimated for various hypothetical β
386 values using the 39 stations. The best estimator of the exponent β is achieved for $\beta=-1.5$
387 according to R^2 . The Ln-Ln linear regression relation is reported in Figure 5a. It results in
388 $R^2>0.8$, reflecting a good performance. The alternative of linking mean basin runoff to mean
389 basin rainfall rather than to drainage area (Eq. (1b)) results in $\beta=0.1$ with $P_{ref}=100$ mm as the
390 most appropriate estimation. The Ln-Ln linear regression relation is reported in Figure 5b.

391 The coefficient of determination R^2 is equal to 0.79, which is less satisfactory than the R^2
392 obtained using drainage area (0.89). Thus, we further assume the drainage area as the sole
393 attribute.

394 The scatter plot of the residuals against the explanatory variables (logarithm of drainage
395 areas) is now examined. Figure 5c shows no decrease or increase of residuals with the
396 increase in the logarithm of drainage areas, thus revealing no heteroscedasticity of the
397 variable Z (errors). The resulting values are shown in Table 3.

398 **4.2 Spatial variability results**

399 The residuals of regression estimation of the average specific annual modules Q_N in the 19
400 gauged basins are assumed as a variability pattern Z to be analyzed and to be used to quantify
401 the sample semivariogram. The latter is reported in Figure 6 as well as the size of the samples
402 which are used to derive it.

403 The fitted exponential model is without any nugget effect, displaying a range parameter of 30
404 km and a sill parameter of $1.4 \text{ (m}^3/\text{s/km}^2\text{)}^2$. The fitted spherical model is without any nugget
405 effect, with a range of 50 km and a sill parameter of $1.2 \text{ (m}^3/\text{s/km}^2\text{)}^2$. For these two models,
406 the dependency ratio is equal to 0, which translates a strong spatial dependency in the data.
407 This is well-understood since residual errors originate from regression using mean squares
408 errors with unbiased mean error.

409 The exponential semivariogram model yields satisfactory cross validation results since the
410 standardized errors are all varying in the acceptable interval range $[-2, 2]$ (see Table 3).
411 Besides, the determination coefficient R^2 is equal to 0.72 which is nearly the value obtained in
412 Laaha et al. (2014) for top-kriging ($R^2=0.75$). For the spherical model, the cross-validation
413 results are less convincing than those obtained with the exponential model. For instance, for
414 the Mkhachbia station (O4), the standardized error is less than -2 (see Table 3). Besides, the

415 determination coefficient R^2 is equal to 0.45, namely much lower than that of the exponential
416 model.

417 Thus, the exponential model is adopted as a spatial variability structure since it gives the best
418 results in cross-validation.

419 **4.3 Augmented hydrometric networks results**

420 As presented in the methodology, to achieve the optimization objective, the spatial average
421 kriging variance of the interpolation error Z is minimized over the candidate networks using
422 simulated annealing. As expected, we notice that, as the network size goes up, the estimation
423 average variance goes (Table 4), thus reflecting the increase in spatial interpolation accuracy
424 with the increase in the number of network hydrometric gauges. Moreover, seemingly, the
425 number of additional stations may still go up since the curve relating spatial average kriging
426 variance to the number of additional stations has not reached a sill. In this work, it is assumed
427 a maximum of 5 new stations only because of financial constraints. It seems that this size can
428 be increased as the optimal size of the network has not been reached yet.

429 As an example, Figure 7 shows the spatial distribution of an optimized network for Scenario
430 5. The five new stations are spared between the left and right banks. One basin upstream at
431 the Algerian frontier is selected (C15). Various basin sizes are covered by the selected
432 locations ranging from 209 to 594 km² while the range for the candidate locations is from 107
433 to 755 km². Indeed, the selected stations are distributed adequately around the Medjerda
434 River. It seems that the algorithm operated a synthesis in both upstream and downstream
435 directions, as well as between the left bank and the right bank.

436 The resulting optimal stations obtained from the five scenarios are listed in Table 5. From a
437 scenario to another, it is worth noticing that there is a perfect conformity with regards to the
438 new sites when progressing from 1 to 5 stations. This means that, for a given scenario, the
439 locations of the new sites include the optimal stations which have already been chosen in the

440 previous scenario. This indicates the robustness of the location identification and its practical
441 importance.

442 **4.4 Interpretation**

443 The presentation of the results is as follows: in Scenario 1, the selected station is the candidate
444 C14 located upstream on the Tessa's tributary (right bank) with a 509 square kilometer basin.
445 In Scenario 2, in addition to station C14, the optimization indicates that a station (C4) should
446 be implemented downstream in Lahmar tributary (right bank) for a 594 square kilometer
447 basin. In Scenario 3, the previously selected stations (C14 and C4) are also reselected and the
448 third location is recommended on Beja tributary, on the left bank (candidate C5) with 209
449 square kilometer basin. In Scenario 4, the selection of the previous stations (C14, C4 and C5)
450 is confirmed and the fourth station is recommended on the Rmil tributary of Siliana River in
451 the right bank (C7) for a 277 square kilometer basin. Finally, in Scenario 5, the four previous
452 recommended stations (C14, C4, C5 and C7) are maintained with an additional basin C15 on
453 the left bank, located on a Medjerda's tributary at the Algerian frontier with a 245 square
454 kilometer drainage area. This last new station is proposed for the upper stream near the river
455 course, far from the first four selections.

456 What are the implications of the findings with respect to the average inter-station distance,
457 average drainage area as well as minimum and maximum inter-stations distances?

458 Table 5 reports the average inter-station distances as well as the average drainage area for
459 each scenario, together with the minimum and maximum inter-stations distances. The lowest
460 minimum inter-stations distance (about 11 km) is given by the initial network of 12 stations.

461 As no candidate is proposed with a smaller inter-distance, the minimum remains unchanged.

462 For Scenario 1 (adding one single station), maximum inter stations distance remains that
463 given by the initial network of 12 stations (about 168 km). In fact, this maximum value is the
464 distance between Mkhachbia and Mellegue K13 basins (from respectively the East side and

465 the West side of the Medjerda basin). Figure 8 shows the progression in mean centroids inter-
466 distances. The algorithm decreases the basin inter-distances when selecting one new location
467 (Scenario 1). This insures a better spatial coverage. The addition of two best locations to the
468 initial network is achieved in order to extend the network, which is reflected by the
469 augmentation of the maximum basins inter-distance (Figure 8). The increase of a maximum
470 inter-distance is achieved together with an increase in mean inter-distance in Scenario 2.
471 From Scenario (3) to Scenario (5) the average inter-station distance is increased and then
472 decreased (Table 5), while conversely, the mean drainage area is regularly decreased from
473 Scenario (1) to Scenario (5) (Table 5). This shows that the optimized networks keep
474 candidates that shift the average drainage area of the optimized network towards higher
475 specific discharges ranges.

476 **5. Conclusions**

477 An approach based on geo-regression combined to ordinary kriging of log specific runoff
478 versus log drainage area residuals is adopted to extend a hydrometric network in order to
479 evaluate an important hydrological descriptor, the average specific annual module, more
480 accurately. To achieve the optimization objective, the spatial average kriging variance of the
481 kriging interpolation error is considered. The kriged variable is the error of estimation of the
482 normalized (scaled) average specific discharge by regression using drainage area.

483 The minimization of the objective function represented by the mean areal variance of kriging
484 error is achieved by using simulated annealing.

485 The Northern region of Tunisia, which has a sub-humid to semi-arid climate, is used in order
486 to develop the methodology. The approach is based on the evaluation of five scenarios for
487 augmenting the size of an initial network of 12 stations. The analysis of the optimized
488 locations from a scenario of one single additional station to five additional stations shows a
489 perfect agreement in relation to the new sites' location. Actually, the locations of the new sites

490 include the optimal stations already chosen in the previous scenarios. The new locations
491 insure a better spatial coverage of the study area as seen from the increase of the average and
492 the maximum inter-station distances after optimization. The results also show that the
493 optimized networks introduce basins that insure the shifting of the mean drainage area
494 towards higher specific discharges ranges. There is no limitation to apply this kind of study
495 elsewhere provided that a significant link exists between the drainage area and the specific
496 mean runoff, and also, provided that a scaling formula may be fitted. In the absence of a
497 significant link between the drainage area and the specific discharge, other proxy variables
498 should be selected. If the scaling formula could not be fitted for the whole study area, a
499 regionalization of the scaling formula is recommended. The type of semivariogram model
500 (exponential) selection is not considered as a limitation. In fact, the only limitation is that the
501 optimization should be performed in accordance with the range of the semivariogram (the
502 location of the new sites must respect the de-correlation distance of the fitted semivariogram).
503 The perspectives in research topics aim to develop a multi-objective optimization problem so
504 that it can include the financial concerns and the optimal size of the network. Besides, the
505 method of Particle swarm optimization (Taormina and Chau, 2015) is proposed as a
506 perspective for the optimization algorithm.

507 **REFERENCES**

- 508 Acreman, M.C., Sinclair, C.D., 1986. Classification of drainage basins according to their
509 physical characteristics; an application for flood frequency analysis in Scotland. *J.*
510 *Hydrol.* 84, 365–380.
- 511 Adamowski, K., Bocci, C., 2001. Geostatistical regional trend detection in river flow data,
512 *Hydrol. Processes.* 15, 3331–3341.
- 513 ASTER Global Digital Elevation Map Announcement, 2012.
514 <https://asterweb.jpl.nasa.gov/gdem.asp>.

515 Barca, E., Passarella, G., Uricchio, V., 2008. Optimal extension of the rain gauge monitoring
516 network of the Apulian Regional Consortium for Crop Protection. *Environ Monit*
517 *Assess.* 145, 375–386.

518 Bardossy, A., 1997. Introduction to geostatistics. Technical report, Institute for Hydraulic
519 Engineering and Water Resources Management, University of Stuttgart.

520 Bozdogan, H., 2000. Akaike's information criterion and recent developments in informational
521 complexity. *Journal of Mathematical Psychology.* 44, 62–91.

522 Bum, D.H., Goulter, I.C., 1991. An approach to the rationalization of streamflow data
523 collection networks. *Journal of Hydrology.* 122, 71–91.

524 Cambardella, C.A., Moorman, T.B., Novak, J.M., Parkin, T.B., Karlen, D.L., Turco, R.F.,
525 Konopka, A.E., 1994. Field-scale variability of soil properties in central Iowa soils. *Soil*
526 *Science Society of America Journal.* 58, 1501–1511.

527 Caselton, W.F., Husain, T., 1980. Hydrologic network: Information transmission. *J. of Water*
528 *Resour. Plan. and Manag. Div.* 106(2), 503–520.

529 Castellarin, A., 2007. Probabilistic envelope curves for design flood estimation in ungauged
530 sites. *WRR* 43(4), W04406 1–12.

531 Chebbi, A., Kebaili Bargaoui, Z., Da Conceição Cunha, M., 2011. Optimal extension of rain
532 gauge monitoring network for rainfall intensity and erosivity index interpolation.
533 *Journal of Hydrologic Engineering.* 16(8), 665–676.

534 Chebbi, A., Kebaili Bargaoui, Z., Da Conceição Cunha, M., 2013. Development of a method
535 of robust rain gauge network optimization based on intensity-duration-frequency results.
536 *Hydrology and Earth System Sciences.* 17, 4259–4268.

537 Cressie, N.A.C., 1993. *Statistics for Spatial Data, (Revised Edition).* Wiley: New York.

538 Cunha, M.C., 1999. On solving aquifer management problems with simulated annealing
539 algorithms. *Water Resources Management.* 13, 153–169.

540 Daigle, A., St-Hilaire, A., Beveridge, D., Caissie, D., Benyahya, L., 2011. Multivariate
541 analysis of the low-flow regimes in eastern Canadian rivers. *Hydrological Sciences*
542 *Journal*. 56(1), 51–67.

543 Davar, Z.K., Brimley, W.A., 1990. Hydrometric network evaluation: Audit approach, J.
544 *Water Resour. Plann. Manage.* 116, 134–146.

545 Daviau, J-L., Adamowski, K., Patry, G.G., 2000. Regional flood frequency analysis using
546 GIS, L-moment and geostatistical methods. *Hydrol. Processes*. 14, 2731–2753.

547 Eaton, B., Church, M., Ham, D., 2002. Scaling and regionalization of flood flows in British
548 Columbia, Canada. *Hydrol. Processes*. 16, 3245–3263.

549 Fair, R.C., 1986. Chapter 33 Evaluating the predictive accuracy of models. *Handbook of*
550 *Econometrics*. 3, 1979–1995.

551 Fleischer, M.A., 1995. Simulated annealing: past, present, and future. In: C. Alexopoulos, K.
552 Kang, W.R. Lilegdon and D. Goldsman (eds.), *Proceedings of the 1995 Winter*
553 *Simulation Conference*, IEEE Press, 155–161.

554 Ghorbel, A., 1997. Dynamique fluviale de la Medjerda : Identification des points de
555 débordements depuis le barrage de SIDI SALEM jusqu'à la mer. DGRE, 11 p.

556 Glatzer, E., Muller, W.G., 2004. Residual diagnostics for variogram fitting. *Computers and*
557 *Geosciences*. 30, 859–866.

558 Hundecha, Y., Bardossy, A., 2004. Modeling of the effect of land use changes on the runoff
559 generation of a river basin through parameter regionalization of a watershed model.
560 *Journal of Hydrology*. 292, 281–295.

561 Kirkpatrick, S., Gelatt, C.D., Vecchi, M.P., 1983. Optimization by Simulated Annealing.
562 *Science*. 220(4598), 671–680.

563 Kjeldsen, T.R., Jones, D.A., 2007. Estimation of an index flood in the UK, *Hydrol. Sci. J.* 52,
564 86–98.

565 Kron, W., Willems, W., 2002. Flood risk zoning and loss accumulation analysis for Germany,
566 International Conference on Flood Estimation, 6–8 March 2002, Berne, Switzerland,
567 pp. 549–558.

568 Laaha, G., Skøien, J.O., Blöschl, G., 2014. Spatial prediction on river networks: comparison
569 of top-kriging with regional regression. *Hydrol. Process.* 28, 315–324.

570 Lin, G.F., Chen, L.H., 2004. A spatial interpolation method based on radial basis function
571 networks incorporating a semivariogram model. *Journal of Hydrology.* 288, 288–298.

572 Matheron, G., 1970. *Cours de géostatistique, chapitre VI. Notes de cours de DEA.*

573 Merz, R., Blöschl, G., 2005. Flood frequency regionalization—Spatial proximity vs.
574 catchment attributes. *J. Hydrol.* 302, 283–306.

575 Mishra, A.K., Coulibaly, P., 2009. Developments in hydrometric network design: A review.
576 *Reviews of Geophysics.* 47(2), RG2001 / 2009, 1–24.

577 Moss, M.E., Tasker, G.D., 1991. An intercomparison of hydrological network-design
578 technologies. *Hydrological Sciences Journal.* 36, 209–221.

579 Rodier, J.A., Colombani, J., Claude, J., Kallel, R., 1981. *Monographies hydrologiques, le*
580 *bassin de la Medjerdah, ORSTOM, Direction des ressources en eaux et en sols, Division*
581 *des ressources en eau, Service hydrologique de Tunisie, 472p.*

582 Rouhani, S., 1985. Variance reduction analysis. *Water Resources Research.* 21(6), 837–846.

583 Sadegh, M., Vrugt, J.A., Gupta, H.V., Xu, C., 2016. The soil water characteristic as new class
584 of closed-form parametric expressions for the flow duration curve. *Journal of*
585 *Hydrology.* 535, 438–456.

586 Skøien, J.O., Blöschl, G., Western, A.W., 2003. Characteristic space-time scales in
587 hydrology. *Water Resour. Res.* 39(10), 1304.

588 Skøien, J.O., Merz, R., Blöschl, G., 2006. Top-kriging – geostatistics on stream networks.
589 *Hydrol. Earth Syst. Sci.* 10, 277–287.

590 Taormina, R., Chau, K.W., 2015. Data-driven input variable selection for rainfall-runoff
591 modeling using binary-coded particle swarm optimization and Extreme Learning
592 Machines. *Journal of Hydrology*. 529 (3), 1617–1632.

593 Tarboton, D.G., Bras, R.L., Puente, C.E., 1987. Combined hydrologic sampling criteria for
594 rainfall and streamflow, *J. Hydrol.* 95, 323–339.

595 Tasker, G.D., Stedinger, J.R., 1989. An Operational GLS Model for hydrologic regression. *J.*
596 *of Hydrol.* 111(1-4), 361–375.

597 Vivekanandan, N., 2012. Evaluation of Stream Flow Network using Entropy Measures of
598 Normal and Lognormal Distributions. *Bonfring Journal of Industrial Engineering and*
599 *Management Science*. 2(3), 33–37.

600 Vivekanandan, N., 2014. Evaluation of Stream Flow Network Using Entropy. *Current*
601 *Advances in Civil Engineering (CACE)*. 2(3), 90–94.

602 Wilson, J.P., Gallant, J.C., 2000. Digital Terrain Analysis. Chap. 1 in *Terrain Analysis:*
603 *Principles and Applications*.

604 Zahar, Y., Ghorbel, A., Albergel, J., 2008. Impacts of large dams on downstream flow
605 conditions of rivers: Aggradation and reduction of the Medjerda channel capacity
606 downstream of the Sidi Salem dam (Tunisia). *Journal of Hydrology*. 351, 318–330.

607

608

Figure 1

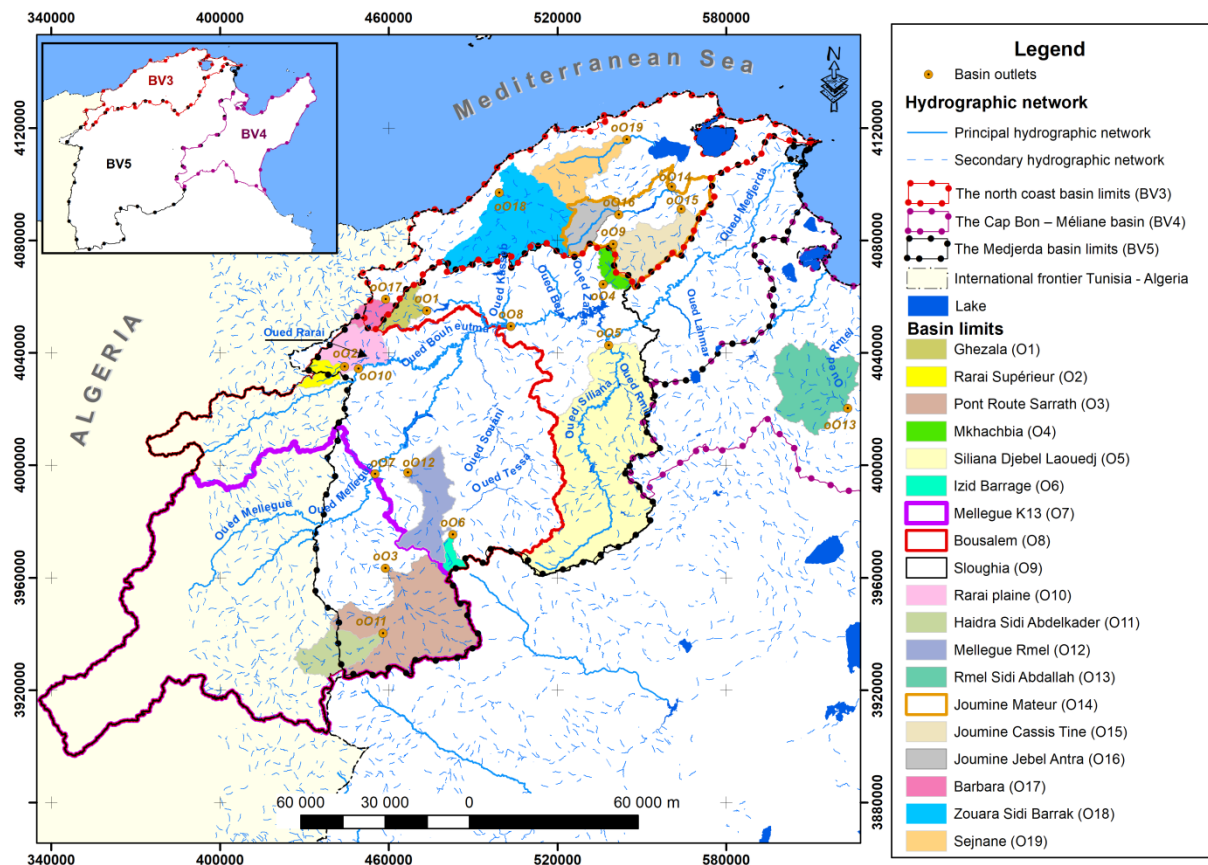


Figure 1. Gauged basin outlets for the 19 stations

Figure 2

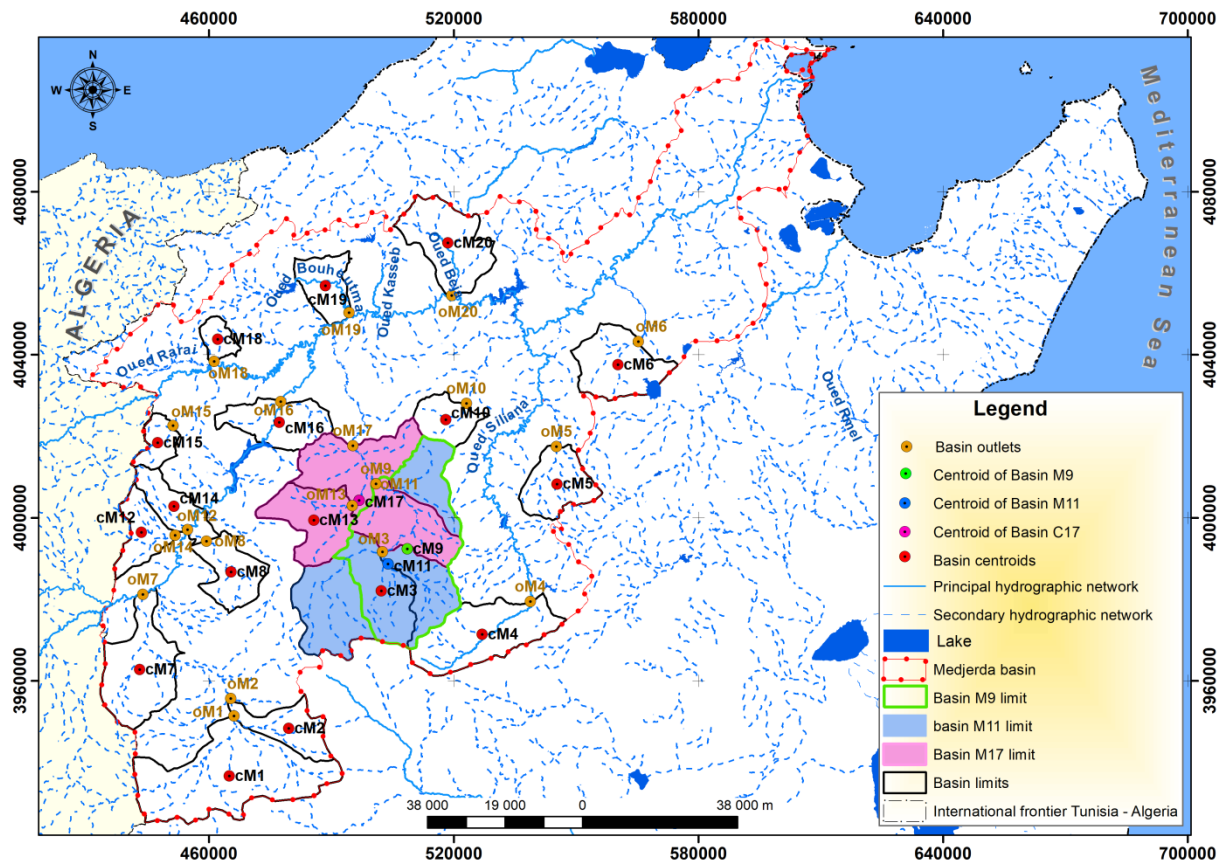


Figure 2. Basins centroids and outlets of “grid” nodes for $M=20$ selected basins

Figure 3

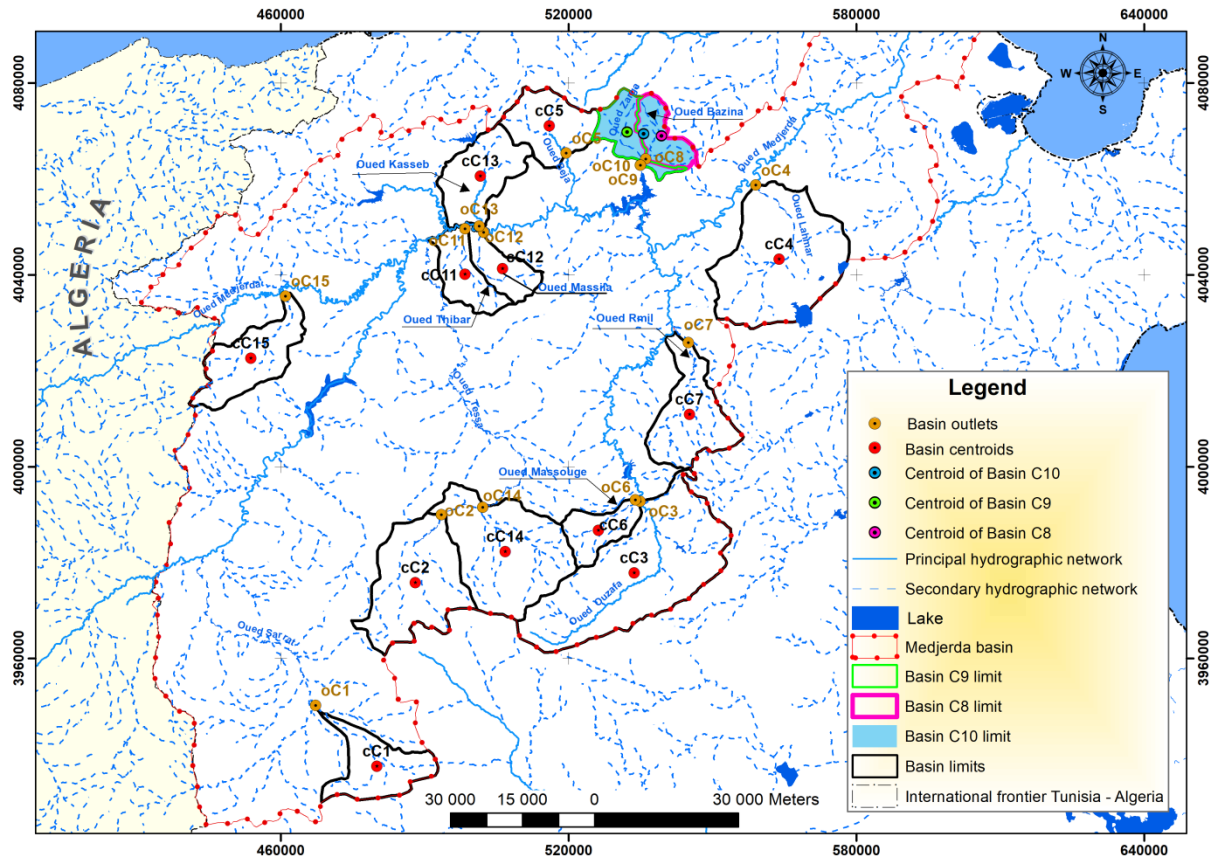


Figure 3. Centroids of the fifteen candidate locations for composing the optimal network

Figure 4

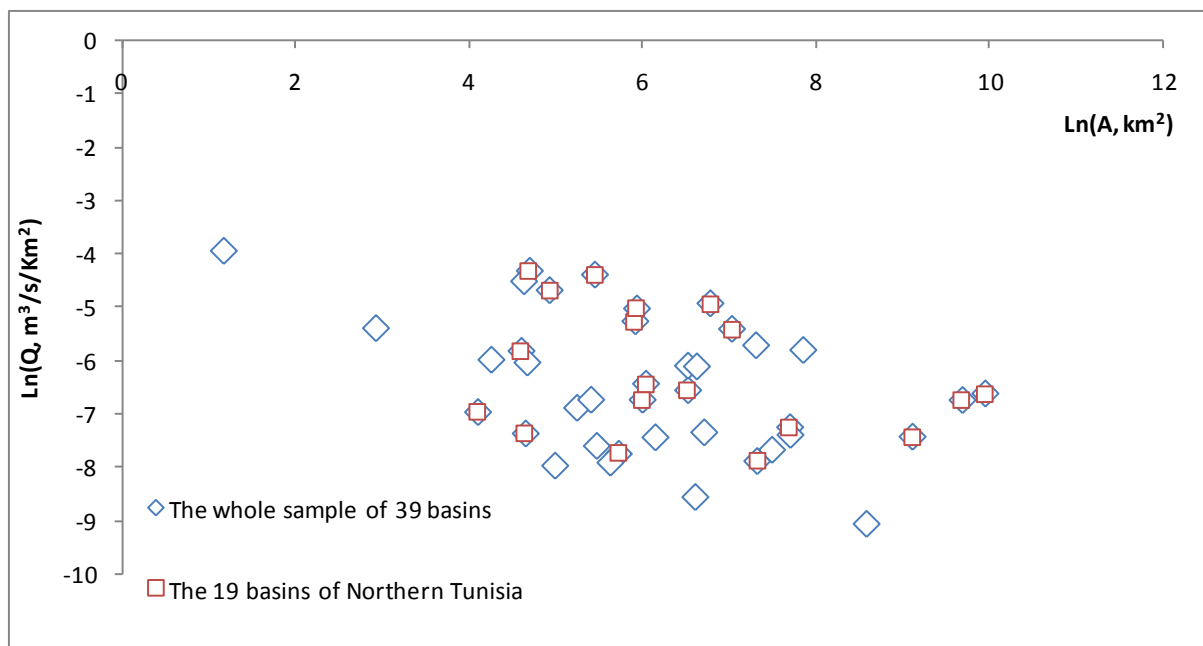


Figure 4. The logarithms of observed average specific annual module versus the logarithms of drainage area

Figure 5

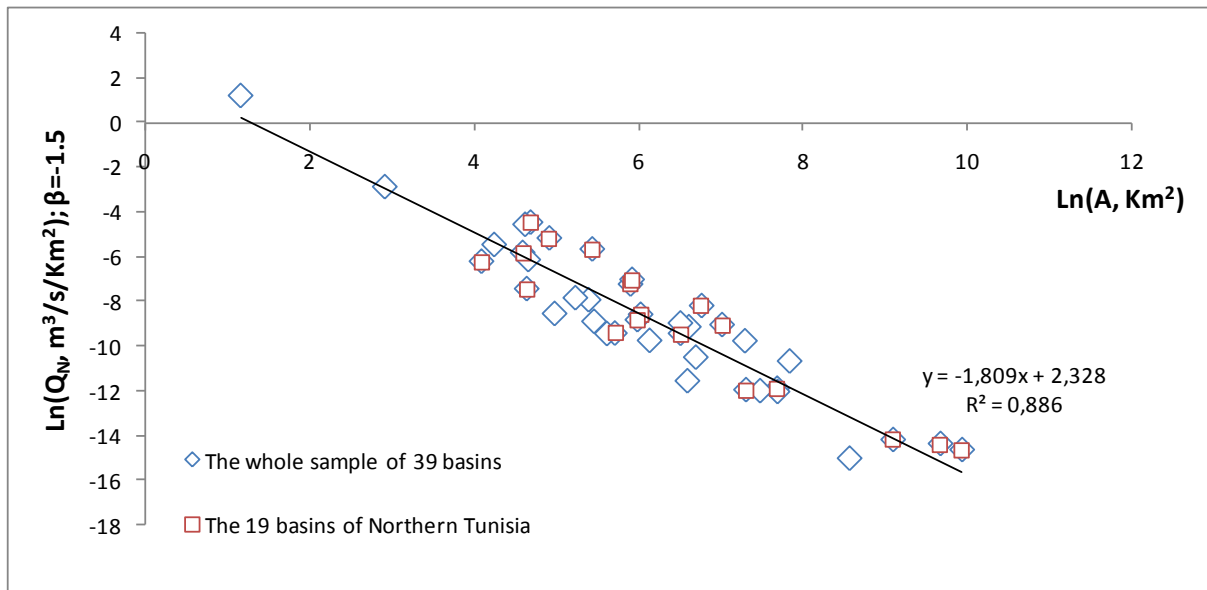


Figure 5a. Linear regression relation between the logarithm of scaled specific discharge Q_N and the logarithm of drainage area A .

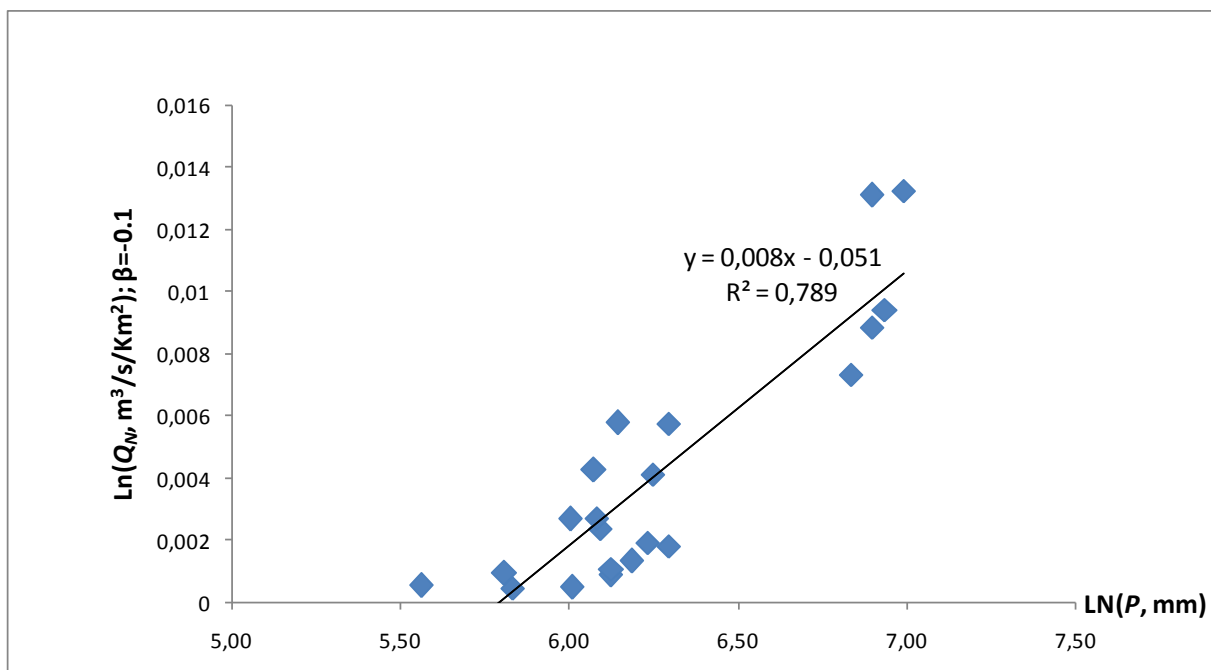


Figure 5b. Linear regression relation between the logarithm of scaled specific discharge Q_N and the logarithm of basin mean rainfall P (for 21 gauged basins with rainfall information)

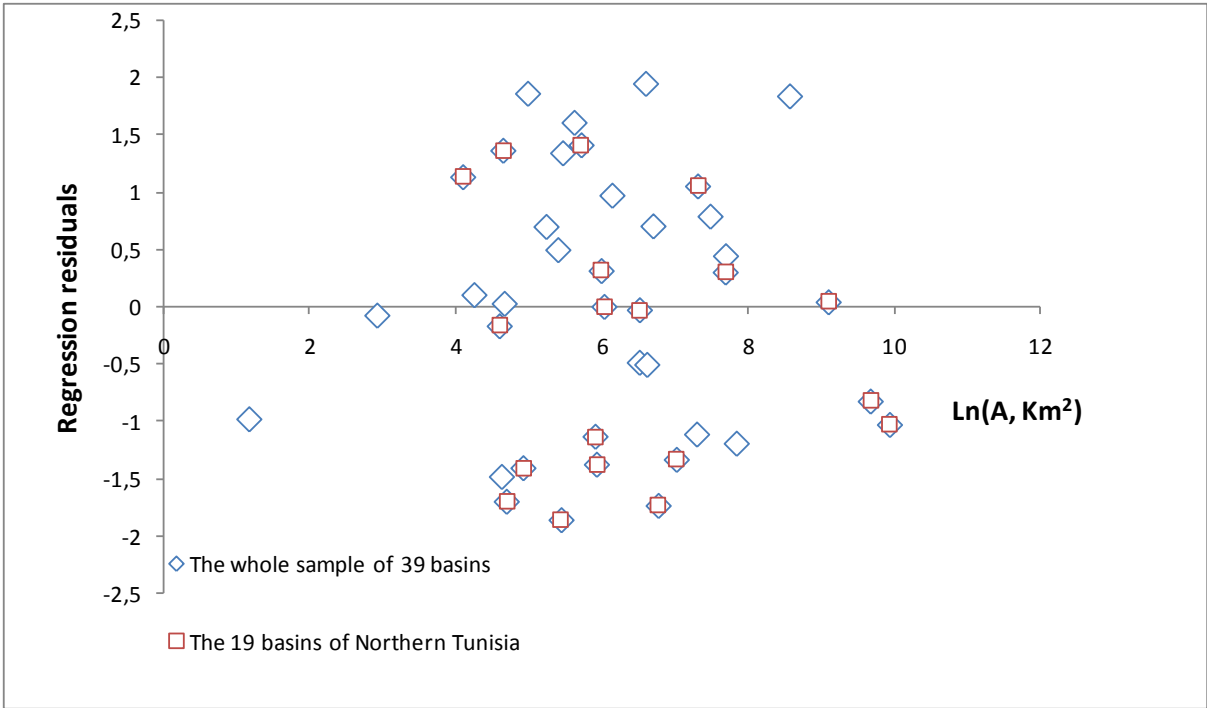


Figure 5c. Regression residuals versus logarithm of drainage areas

Figure 6

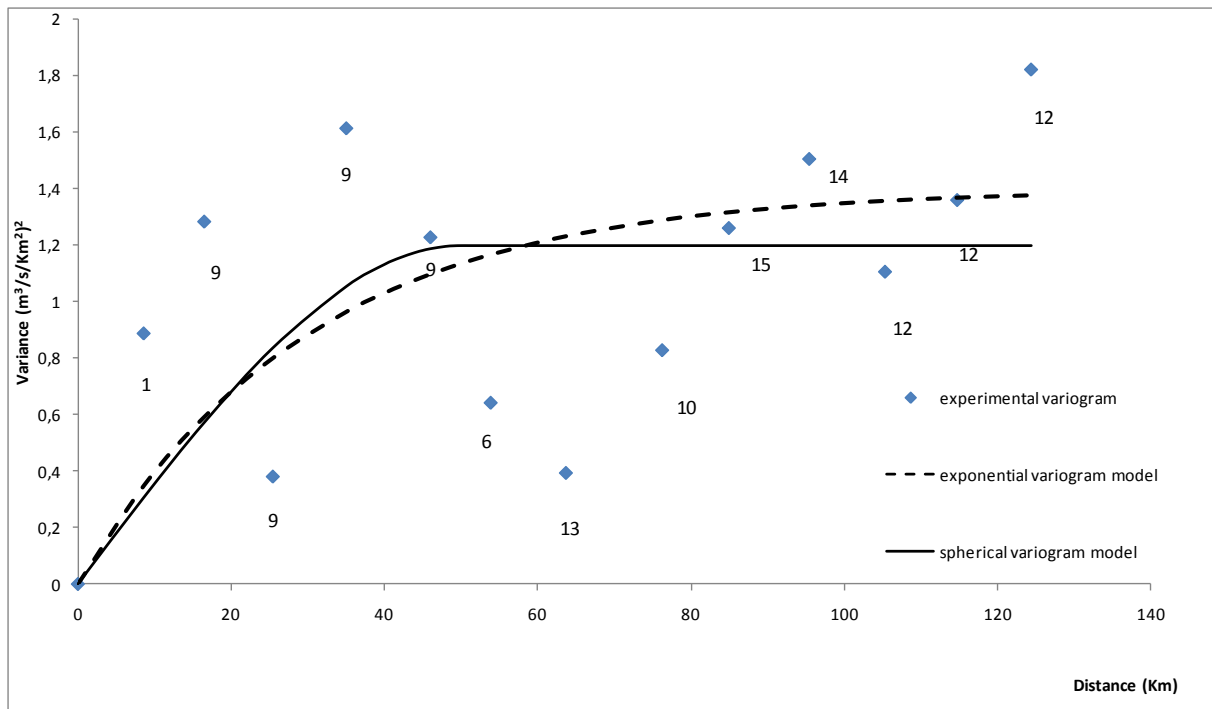


Figure 6. Calibration of the semivariogram of residuals of estimation of the scaled average specific discharge (with the corresponding sample size of pairs)

Figure 7

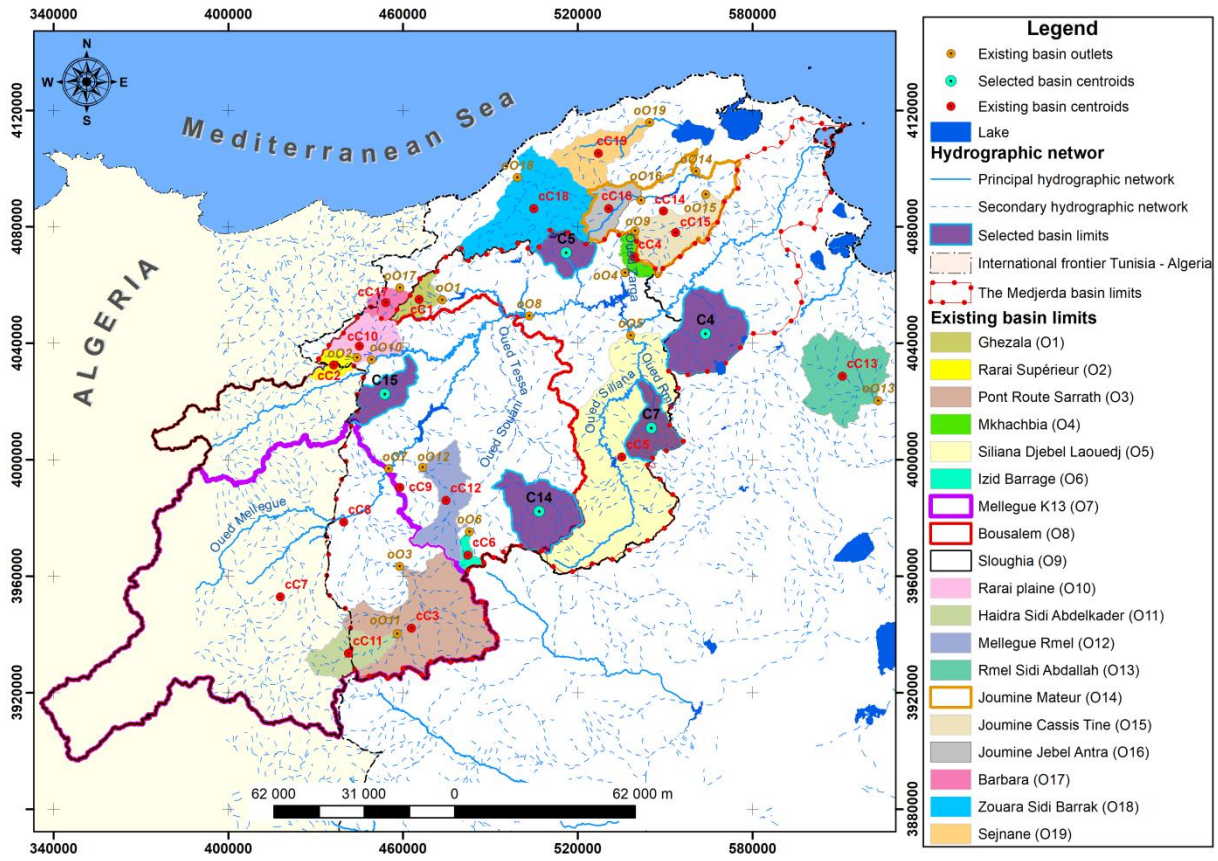


Figure 7. Spatial distribution of the optimized hydrometric network for Scenario 5 with 5 new sites.

Figure 8

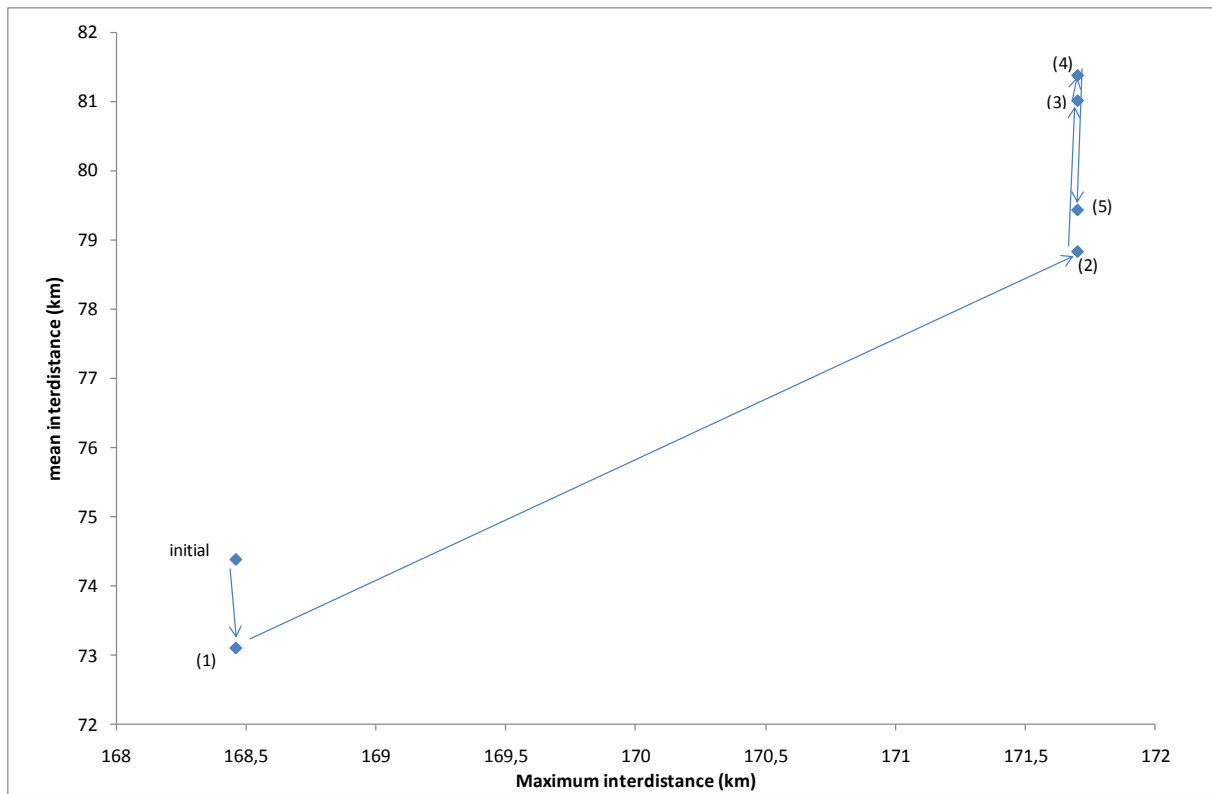


Figure 8. The progression in mean and maximum centroids interdistance according to the Scenario (1) to (5)

Table 1[Click here to download Table: Table 1.docx](#)

Table 1. Presentation of the 19 hydrometric stations of the study area

Station name	Basin	Station Code in Fig. 1	Drainage area (km ²)	Average annual module (m ³ /s)
Ghezala in Bouheurtma basin	BV5	O1	137	1.25
Rarai Supérieur in Rarai basin	BV5	O2	99	0.29
Pont Route Sarrath in Mellegue basin	BV5	O3	1500	0.56
Mkhachbia in Mkhachbia basin	BV5	O4	104	0.06
Siliana Djebel Laouedj in Siliana basin	BV5	O5	2191	1.54
Izid Barrage in Tessa basin	BV5	O6	60	0.06
Mellegue K13 in Mellegue basin	BV5	O7	8988	5.29
Bousalem along the Medjerda river	BV5	O8	15993	18.70
Sloughia along the Medjerda river	BV5	O9	20811	27.50
Rarai plaine in Rarai basin	BV5	O10	368	1.88
Haidra Sidi Abdelkader in Mellegue basin	BV5	O11	304	0.13
Mellegue Rmel in Mellegue basin	BV5	O12	400	0.47
Rmel Sidi Abdallah in Rmel basin, BV4	BV4	O13	676	0.95
Joumine Mateur in Joumine basin	BV3	O14	1121	4.96
Joumine Cassis Tine in Joumine basin	BV3	O15	416	0.66
Joumine Jebel Antra in Joumine basin	BV3	O16	231	2.82
Barbara in Barbara basin	BV3	O17	109	1.43
Zouara Sidi Barrak in Zouara basin	BV3	O18	874	6.24
Sejnane in Sejnane basin	BV3	O19	375	2.43

Table 2[Click here to download Table: Table 2.docx](#)

Table 2. Presentation of the 15 candidate stations (area, tributary and location). RB: right bank, LB: left bank of Medjerda river

Station code	Drainage area (km ²)	Name of the tributary and description of location
C1	214	In upstream Sarrat river, in Mellegue basin, RB
C2	419	On Tessa river, RB
C3	755	On Ouzafa river, tributary of Siliana river, RB
C4	594	On Lahmar river, RB
C5	209	On Beja river, LB
C6	124	On Massouge river, tributary of Siliana river, RB
C7	277	On Rmil river, tributary of Siliana river, RB
C8	107	On Bazina river, tributary of Zarga river, LB
C9	112	On Zerga river, LB
C10	219	On Zerga river, LB
C11	147	On Massila river, LB
C12	116	On Thibar river, RB
C13	236	On Kasseb river, LB
C14	503	On Tessa river, RB
C15	245	Ezana direct tributary of the Medjerda basin, at the Algerian boundary, LB

Table 3[Click here to download Table: Table 3.docx](#)

Table 3. Error for the selected variogram and cross-validation results: the standardized errors at the 19 stations of the study area

Station name	Station Code	Error Z for the selected variogram ($m^3/s/Km^2$)	For the exponential model	For the spherical model
Ghezala in Bouheurtma basin	O1	-1.40	0.68	0.10
Rarai Supérieur in Rarai basin	O2	-0.17	-0.47	-0.74
Pont Route Sarrath in Mellegue basin	O3	1.05	-0.48	-0.38
Mkhachbia in Mkhachbia basin	O4	1.36	-1.71	-2.44
Siliana Djebel Laouedj in Siliana basin	O5	0.30	-0.29	-0.60
Izid Barrage in Tessa basin	O6	1.13	-0.56	-0.84
Mellegue K13 in Mellegue basin	O7	0.040	0.25	0.12
Bousalem along the Medjerda river	O8	-0.82	-0.61	0.33
Sloughia along the Medjerda river	O9	-1.03	1.17	0.98
Rarai plaine in Rarai basin	O10	-1.13	0.70	0.59
Haidra Sidi Abdelkader in Mellegue basin	O11	1.41	-1.14	-1.12
Mellegue Rmel in Mellegue basin	O12	0.31	-0.79	-0.46
Rmel Sidi Abdallah in Rmel basin, BV4	O13	-0.03	0.20	-0.38
Joumine Mateur in Joumine basin	O14	-1.33	0.86	1.32
Joumine Cassis Tine in Joumine basin	O15	0.00	-0.46	-0.65
Joumine Jebel Antra in Joumine basin	O16	-1.86	0.80	1.41
Barbara in Barbara basin	O17	-1.70	-0.26	0.60
Zouara Sidi Barrak in Zouara basin	O18	-1.73	0.48	0.83
Sejnane in Sejnane basin	O19	-1.37	-0.72	-0.31

Table 4[Click here to download Table: Table 4.docx](#)

Table 4. Reduction of uncertainty by increase of network density

Increasing the existing network by	spatial average kriging variance ($\text{m}^3/\text{s}/\text{km}^2$) ²
Initial 12 stations network	0.92
1 new station	0.82
2 new stations	0.78
3 new stations	0.73
4 new stations	0.70
5 new stations	0.67

Table 5[Click here to download Table: Table 5.docx](#)

Table 5. Optimal solutions for the five scenarios and corresponding interdistances

Increasing the existing network by	Code of the selected candidate(s)	Minimum interdistance (km)	Maximum interdistance (km)	Mean interdistance (km)	Mean drainage area (km ²)
Initial network		10.9	168.5	74.4	4246
1 new station	{C14}	10.9	168.5	73.1	3958
2 new stations	{C14, C4}	10.9	171.7	78.8	3718
3 new stations	{C14, C4, C5}	10.9	171.7	81.0	3484
4 new stations	{C14, C4, C5, C7}	10.9	171.7	81.4	3284
5 new stations	{C14, C4, C5, C7, C15}	10.9	171.7	79.4	3105

Figure captions

Figure 1. Gauged basin outlets locations for the 19 stations

Figure 2. Basins centroids and outlets of “grid” nodes for $M=20$ selected basins

Figure 3. Centroids of the fifteen candidate locations for composing the optimal network

Figure 4. The logarithms of observed average specific annual module versus the logarithms of drainage area

Figure 5a. Linear regression relation between the logarithm of scaled specific discharge Q_N and the logarithm of drainage area A .

Figure 5b. Linear regression relation between the logarithm of scaled specific discharge Q_N and the logarithm of basin mean rainfall P (for 21 gauged basins with rainfall information)

Figure 5c. Regression residuals versus logarithm of drainage areas

Figure 6. Calibration of the semivariogram of residuals of estimation of the scaled average specific discharge (with the corresponding sample size of pairs)

Figure 7. Spatial distribution of the optimized hydrometric network for Scenario 5 with 5 new sites.

Figure 8. The progression in mean and maximum centroids interdistance according to the Scenario (1) to (5)